Glycoconj J (2012) 29:399–409
DOI 10.1007/s10719-012-9408-z

Site-specific N-glycosylation identification of recombinant human lectin-like oxidized low density lipoprotein receptor-1 (LOX-1)

Yifan Qian · Xingwang Zhang · Lei Zhou · Xiaojing Yun · Jianhui Xie · Jiejie Xu · Yuanyuan Ruan · Shifang Ren

Received: 15 April 2012 / Revised: 24 May 2012 / Accepted: 29 May 2012 / Published online: 12 June 2012

Abstract Human LOX-1/OLR 1 plays a key role in atherogenesis and endothelial dysfunction. The N-glycosylation of LOX-1 has been shown to affect its biological functions *in vivo* and modulate the pathogenesis of atherosclerosis. However, the N-glycosylation pattern of LOX-1 has not been described yet. The present study was aimed at elucidating the N-glycosylation of recombinant human LOX-1 with regard to N-glycan profile and N-glycosylation sites. Here, an approach using nonspecific protease (Pronase E) digestion followed by MALDI-QIT-TOF MS and multistage MS (MS^3) analysis is explored to obtain site-specific N-glycosylation information of recombinant human LOX-1, in combination with glycan structure confirmation through characterizing released glycans using tandem MS. The results reveal that N-glycans structures as well as their corresponding attached site of LOX-1 can be identified simultaneously by direct MS analysis of glycopeptides from non-specific protease digestion. With this approach, one potential glycosylation site of recombinant human LOX-1 on Asn_{139} is readily identified and found to carry heterogeneous complex type N-glycans. In addition, manual annotation of multistage MS data utilizing diagnostic ions, which were found to be particularly useful in defining the structure of glycopeptides and glycans was addressed for proper spectra interpretation. The findings described herein will shed new light on further research of the structure-function relationships of LOX-1 N-glycan.

Keywords LOX-1 · Site-specific N-glycosylation · Unspecific proteolysis · MALDI-QIT-TOF-MS · Multistage MS

Abbreviations

ACN	Acetonitrile
Asn	Asparagine
Asp	Aspartate
DHB	2 5-dihydroxybenzoic acid
DTT	Dithiothreitol
ESI	Electrospray ionization
Fuc	L-fucose
Gal	D-galactose
GlcNAc	*N*-acetyl-D-glucosamine
Hex	Hexose
HexNAc	*N*-acetylhexosamine
IAA	Iodacetamide
LOX-1	Lectin-like oxidized low density lipoprotein receptor-1
MALDI	Matrix assisted laser desorption/ ionization
Man	D-mannose
MS	Mass spectrometry
PGC	Porous graphic carbon
PNGase F	Peptide N-Glycosidase F
QIT	Quadropole ion trap
RT	Room temperature

Electronic supplementary material The online version of this article (doi:10.1007/s10719-012-9408-z) contains supplementary material, which is available to authorized users.

Y. Qian · X. Zhang · L. Zhou · X. Yun · J. Xie · J. Xu · Y. Ruan · S. Ren
Key Laboratory of Glycoconjugate Research Ministry of Public Health, Shanghai Medical College, Fudan University, Shanghai 200032, People's Republic of China

Y. Qian · X. Zhang · L. Zhou · X. Yun · J. Xie · J. Xu · Y. Ruan · S. Ren (✉)
Department of Biochemistry and Molecular Biology, Shanghai Medical College, Fudan University, Shanghai 200032, People's Republic of China
e-mail: renshifang@fudan.edu.cn

SDS-PAGE	Dodecyl sulfate sodium salt-polyacrylamide gel electrophoresis
SPE	Solid-phase extraction
TFA	Trifluoroacetic acid
TOF	Time of flight
v/v	Volume/volume
w/w	Weight/weight

Introduction

Oxidized low density lipoprotein (Ox-LDL) has been suggested to play key roles in pathogenesis of atherosclerosis and endothelial dysfunction [1, 2]. LOX-1 (lectin-like oxidized low density lipoprotein receptor-1) is a type II membrane protein belonging to the C-type lectin family [3]. N-Linked glycosylation of LOX-1 appears to regulate, at least in part, the intracellular transport and ligand binding of LOX-1. Thus, altered glycosylation of LOX-1 may affect its biological functions *in vivo* and modulate the pathophysiology of diseases including atherosclerosis [4]. The primary sequence of LOX-1 contains two potential N-linked glycosylation sites (Supplemental Table 1). As far as we know, in spite of its significant role in the pathogenesis of atherosclerosis, the glycosylation of LOX-1 has not been determined yet.

Glycosylation is one of the most common post-translational protein modifications whereby glycans are added to the protein chain [5]. Glycoproteins have diverse functions and play a crucial role in many biological processes, which vary from conformational stability, protection against degradation to molecular and cellular recognition in development, growth, and cellular communication [6, 7]. A wide range of diseases have also been associated with abnormalities in carbohydrate degradation and recognition [8, 9]. Therefore, the characterization of glycosylation is particularly important for us in understanding the structure-biological function relationships of glycoproteins.

In this study, we employed a MALDI MS-based method to facilitate glycosylation characterization of recombinant human LOX-1 at the level of intact glycopeptides. Glycopeptide analysis benefits the identification of site-specific glycosylation properties, while the routine method by analysis of released N-glycans usually loses the glycan-protein linkage and site-specific heterogeneity information of glycoproteins [10–12]. And this method is favorable especially when there is more than one oligosaccharide attached to their backbone ruling out the possibility to correlate the changes in glycan structure to a particular site if only released glycans are analyzed [13].

In most cases, the glycoprotein is digested with specific protease, such as trypsin to obtain glycopeptides carrying individual glycosylation sites. However, tryptic digestion of glycoproteins sometimes suffers from the limitation that the glycopeptides of interest are too large in size (mass contribution from glycans and amino acid sequence) and carrying too many heterogeneous modifications to analyze efficiently by mass spectrometry [14–17]. In case of human LOX-1, the theoretical masses of tryptic peptides containing two potential glycosylation sites are 5803.89 Da and 3576.94 Da, respectively (Supplemental Table 1), regardless of the N-glycans masses, which are close to the upper mass limit of ordinary MALDI MS/MS facilities. Furthermore, the larger glycopeptide mass is, the more difficult it is to acquire MS/MS fragmentation spectra with sufficient high quality for unambiguous identification of glycosylation sites [14, 18].

Pronase E is a nonspecific endo-protease that can cleave at every peptide bond theoretically. But due to the steric hindrances, the amino acids adjacent to the glycosylation site(s) are ineffectively cleaved by the enzyme. As a result, a series of short glycopeptides for a given glycosylated site and small nonglycopeptides (<4 amino acids) are generated, which can overcome the limitations of tryptic digestion mentioned above [19]. Some methods employing this nonspecific protease have also been reported for the determination of glycosylation microheterogeneity [14, 20–22]. However, most of these methods were applied to standard glycoprotein with known glycosylation but rarely used in determining the unknown glycosylation of certain glycoprotein. Moreover, using these methods, the peptide moiety of glycopeptides was usually identified by subtracting the masses of the glycans derived from PNGase F treatment from the masses of the glycopeptides, which may cause incorrect peptide sequence assignment. This can be improved if multistage MS like MS^3 is accessible because the peptide can be selected for further fragmentation and thereby generate sequence information for correct glycosylation site assignment. In addition, due to the complexity of glycan structure, MALDI MS spectra dominated with singly charged ions, which simplify the mass spectra, is favorable of data interpretation, comparing with ESI MS spectra, which are often complicated by different multiple-charged ions.

Thus, in our work, a nonspecific proteolysis using Pronase E coupled with MALDI multistage MS was employed together to reveal unknown glycosylation pattern of recombinant human LOX-1. Meanwhile, glycan structures deduced from intact glycopeptides analysis were further validated by characterization of released glycans from PNGase F treatment with tandem MS. The experimental procedure is shown in Chart 1.

Materials and methods

Nonspecific protease digestion of LOX-1

Fifty pmol recombinant LOX-1 (expressed in murine myeloma cell line, R&D Sysems, USA) was dissolved in 4 μL 25 mM NH_4HCO_3 (Sigma-Aldrich, Germany) in H_2O (all water used was generated by milli-Q filtration). To this solution 6 μL 10 mM DTT (Sigma-Aldrich, Germany) was added and

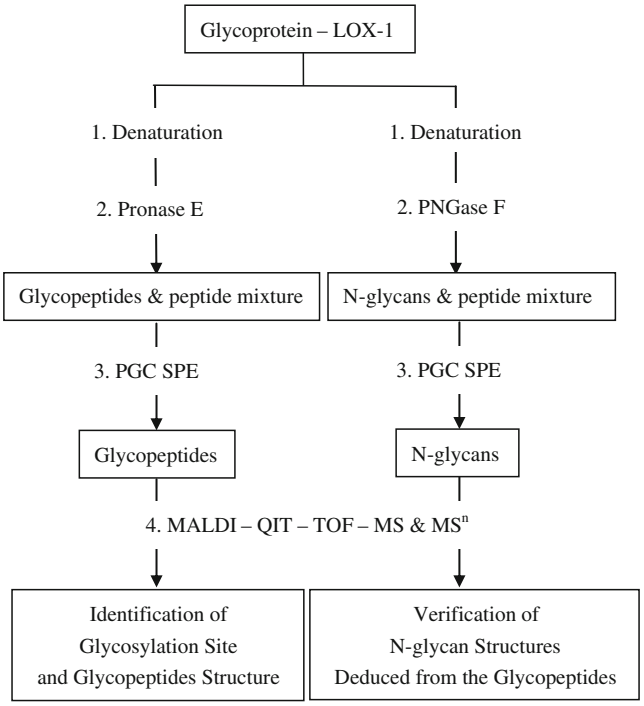

Chart 1 The procedure of site-specific characterization of glycoproteins

the glycoprotein was reduced at 56 °C for 60 min. After cooling to RT, 12 μL 100 mM IAA (Sigma-Aldrich, Germany) was added and the glycoprotein was alkylated for 45 min at RT in the dark. Subsequently, Pronase E (dissolved in ice-cold 25 mM NH_4HCO_3, 0.1 μg/μL) was added to the solution at an enzyme/substrate ratio of 1:10 (*w/w*) and then incubated at 37 °C overnight. Non-reduced digestion was performed as the recombinant LOX-1 without reduction and alkylation was directly incubated with Pronase E at an enzyme/substrate ratio of 1:10 (*w/w*) at 37 °C overnight. The digests were stopped and stored at −20 °C until PGC SPE desalting and purification.

N-glycan release

N-glycans from LOX-1 were released by incubating with PNGase F (New England Biolabs, Inc., USA) in 25 mM NH_4HCO_3 for 12 h at 37 °C.

Glycopeptide and oligosaccharide purification using a microcolumn with porous graphic carbon (PGC-SPE)

Pronase E-digested glycopeptides and PNGase F released oligosaccharides were purified by PGC-SPE using a microcolumn, which was packed with porous graphic carbon powder and prepared using GELoader tips as described previously [23, 24]. The PGC microcolumn was washed 5 times with 25 μL of 0.05 % (*v/v*) TFA in 80 % ACN (acetonitrile)/H_2O (*v/v*) and followed by 0.05 % (*v/v*) TFA in H_2O. The solution of digested glycoprotein or oligosaccharide was applied to the PGC microcolumn repeatedly for 5 times to allow glycoconjugate adsorption. Subsequently, the microcolumn was washed 3 times with 25 μL H_2O to remove salts and buffer. Glycopeptides and glycans were eluted with 40 % ACN in 0.05 % TFA in H_2O directly onto a MALDI plate for analysis.

SDS-PAGE electrophoresis

Gels containing 10 % acrylamide (separating) and 5 % acrylamide (stacking) were prepared and equivalent amounts of LOX-1 and deglycosylated LOX-1 were loaded per lane. Protein standards (PageRuler™ Prestained Protein Ladder, Takara Co., Ltd., Japan) were included. For visualization, gels were stained with Coomassie blue.

In-gel PNGase F and subsequent tryptic digestion

The band of interest was excised from the gel and rinsed three times with Milli-Q water. The band was then cut into approximately 1 mm^2 pieces and dried. The gel slices were reduced with 30 μL 10 mM DTT at 56 °C for 60 min and cooled down to RT. 60 μL 100 mM IAA was added and the glycoprotein was alkylated for 45 min at RT in the dark. Subsequently, the gel slices were completely dried and added to a PNGase F solution. The mixture was incubated at 37 °C overnight. After the extraction of N-glycans, the gel slices were dried and added to a trypsin solution to incubate at 37 °C overnight. After the reaction was cooled down to RT, the supernatant was removed and saved. The gel was subsequently extracted with 100 μL 0.1 % and 5 % TFA in 50 % ACN by gently mixing and incubation at RT for 15 min, respectively. Each wash was combined with the saved supernatant, and the resulting solution was lyophilizated for further MALDI analysis.

Mass spectrometry

MALDI mass spectrometric analysis was performed on AXIMA Resonance MALDI QIT TOF MS (Shimadzu Corp. JP), equipped with a 337 nm nitrogen laser in positive ion detection. The engineering design and operation of the QIT-TOF have been described in detail elsewhere [25, 26]. 12.5 mg mL^{-1} DHB in 50 % acetonitrile (ACN) in water (*v/v*) containing 0.1 % trifluoroacetic acid (TFA) was used as matrix for AXIMA-QIT MALDI TOF MS; tandem MS fragmentation was achieved by CID using argon (QIT) as the collision gas. MALDI samples in aqueous solution (1 μL) were deposited onto the MALDI plate and allowed to dry in air at ambient temperature. Then, 1 μL matrix solution (DHB, Sigma-Aldrich, Germany) was added onto the sample layer and allowed to dry under ambient conditions. TOFMix™ (LaserBio Labs, France) containing eight peptides calibration standard is used for external calibration of MS.

Results and discussion

Non-specific digestion of LOX-1 and enrichment of glycopeptides by PGC SPE

Many glycoproteins are not susceptible to the traditional trypsin digestion procedure, because the glycosylation sites are not always located close to the cleavage sites of the standard proteolytic enzymes, potentially resulting in glycopeptides that are too large for effective tandem MS [22]. In our circumstance, LOX-1 is just a typical representative of such glycoproteins that are unsusceptible to trypsin digestion. The amino acid sequence for the human LOX-1 gene product was obtained from the Swiss-Prot database with accession number P78380 (Supplemental Chart 1). There are 273 amino acids composing the protein moiety with a molecular mass of 25.5 kDa (monomer). LOX-1 has two potential glycosylation at Asn_{73} and Asn_{139} and the two theoretical glycosylated tryptic peptides can be found in Supplemental Table 1, which are already 3576.94 Da and 5803.89 Da respectively, not including the attached N-glycan moiety masses. These are almost beyond the effective *m/z* detection range of our mass spectrometer.

Therefore, in our study, we utilized a nonspecific protease, Pronase E, to digest LOX-1. Large glycosylated peptide fragments were not present as they were digested to short amino acid sequences while the non-glycosylated peptide fragments were cut into shorter amino acid sequences. Ionic species with *m/z* greater than 1000 were glycopeptides as the oligosaccharide moieties corresponded to at least 800 mass units ($GlcNAc_2Man_3$) [20]. So theoretically the glycopeptide ions should be nicely separated by mass from the relatively short non-glycosylated peptides and without further purification steps. However, due to the low ionization efficiency, the signals of glycopeptides may be suppressed by the high abundance of non-glycosylated peptides [27]. The overlapping of signals derived from glycopeptide ions and non-glycosylated peptide ions may still be observed in spectra. Additionally, incubation with Pronase E at 37 °C may result in peptides derived by auto-proteolysis of the enzyme hampering the analysis of complete corresponding glycopeptide patterns. Consequently, an inevitable enrichment of glycopeptides like micro-PGC SPE was employed, which permitted to overcome the problems of signal suppression, overlapping of peptide and glycopeptide signals as well as of the auto-proteolysis peptides derived from Pronase E [18].

Identification and analyses of glycopeptides in LOX-1 by MALDI-QIT-TOF-MS^3

Figure 1 shows the positive ion mass spectrum of glycopeptides (marked with asterisks) obtained after Pronase E digestion and PGC separation. All of glycopeptides are identified through tandem MS. The site-specific glycosylation pattern can be deduced from these tandem MS data of glycopeptides. To illustrate the structure determination of observed glycopeptides, we selected representive tandem MS spectra of predominant glycopeptide signals for a more detailed description as shown in Fig. 2. Figure 2a shows the fragmentation pattern of a $[M+H]^+$ glycopeptide signal at *m/z* 3507.92 as well as Fig. 2b shows its $[M+Na]^+$ glycopeptide precursor at *m/z* 3529.62, from which we can find fragment ions from oligosaccharides and peptide signals. The glycosylation pattern can be identified by analyzing these diagnostic fragment ions. Considering that the N-glycosylation of LOX-1 is unknown, we will address manual annotation of N-glycan pattern in detail using diagnostic ions in MS^2 and MS^3 spectra.

Glycosylation site determination from multistage MS spectra of glycopeptides

Two different series of fragment ions were observed in both Fig. 2a and b, which can be used to deduce N-glycan and peptide moiety of glycopeptide, individually. In Fig. 2a, the first series (black-colored) of cleavages were at or near the innermost *N*-acetylglucosamine residue, with the peptide moiety attached to all the fragment ions. The most intense signal at *m/z* 1091.40 corresponding to a $[M_{pep}+203+H]^+$ fragment, together with the signal at *m/z* 888.36 revealed a cleavage between the Asn and the first GlcNAc in the core glycan structure. Additionally, the $[M_{pep}+203+146+H]^+$ ion

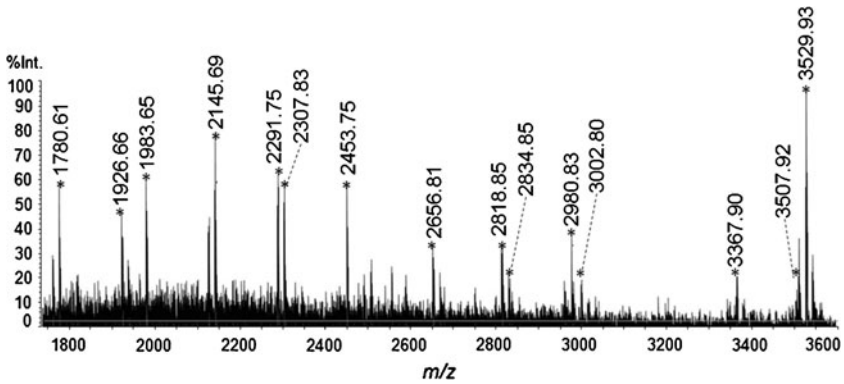

Fig. 1 MALDI-QIT-TOF-MS spectrum of Pronase E-digested glycopeptides of LOX-1

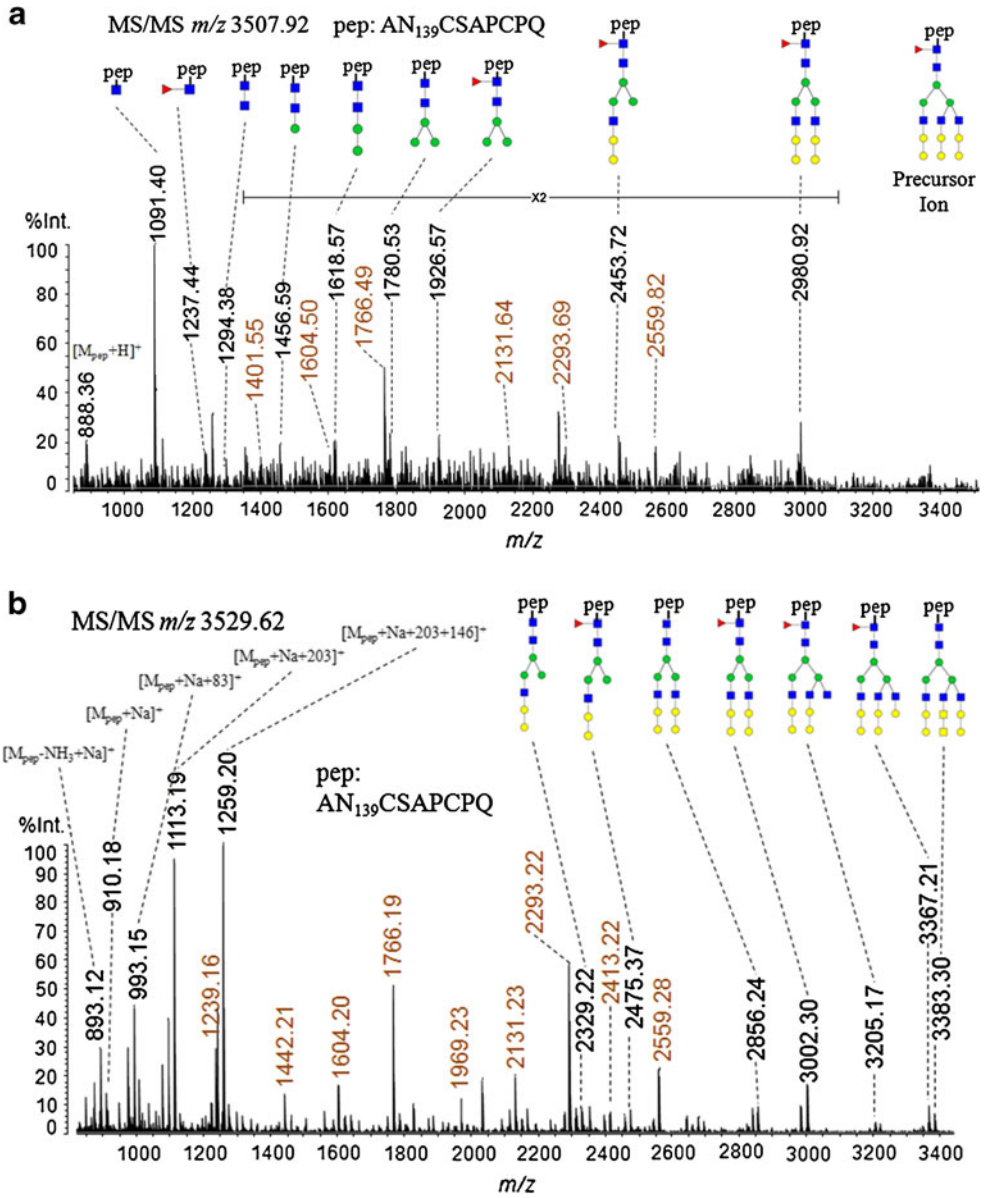

Fig. 2 MS/MS spectra of the Pronase E-digested glycopeptides with complex type structure at *m/z* 3507.92 ($[M+H]^+$) and 3529.62 ($[M+Na]^+$) of LOX-1. The black-colored series of signals corresponds to the glycopeptides (except *m/z* 888.36 $[M_{pep}+H]^+$ in Fig. 2a and *m/z* 893.12 $[M_{pep}-NH_3+Na]^+$, 910.18 $[M_{pep}+Na]^+$ in Fig. 2b), of which the peptide sequence is $AN_{139}CSAPCPQ$. The brown-colored series of signals corresponds to N-glycans of which the structures can be found in Supplemental Table 3 and it should be noted that *m/z* 2413.22 in Fig. 2b corresponds to $[M-146-83-18+Na]^+$

at *m/z* 1237.44 was observed simultaneously, which confirmed that the mass of peptide moiety was 888.36 Da. Similar fragmentation pattern was observed in Fig. 2b: a prominent signal at *m/z* 893.12 corresponds to a $[M_{pep}-NH_3+Na]^+$ fragment, which arises from the cleavage of the side-chain amide bond of the glycosylated asparagine. Additionally, the $[M_{pep}+Na]^+$ ion at *m/z* 910.18 was observed. A $^{0,2}X$-ring cleavage of the innermost *N*-acetylglucosamine generated a $[M_{pep}+Na+83]^+$ ion at *m/z* 993.15. The other two prominent signals at *m/z* 1113.19 and 1259.20 resulted from the Y-type cleavage of the chitobiose core, which correspond to a $[M_{pep}+Na+203]^+$ ion and a $[M_{pep}+Na+203+146]^+$ ion in case of a monofucosylated core, respectively [28]. These typical ions at *m/z* 1259.20, 1113.19, 993.15, 910.18 and 893.12 again verified that the mass of peptide moiety was 888.36 Da.

However, no obvious peptide fragment ions were found in the tandem MS spectra for accurate glycosylation site assignment. It is also reported before that utilizing a non-specific enzyme may in some cases result in difficulties in assignment of the correct peptide sequence even though the sequence of the protein is known [18]. In the present work, the characteristic ion at *m/z* 888.36 was selected as precursor ion for MS^3 in order to gain the information about peptide sequence [29]. Figure 3 shows the MS^3 spectrum of the $[M_{pep}+H]^+$ ion at *m/z* 888.36. From the acquired MS^3 spectrum (Fig. 3), the b-ions and y-ions derived from the peptide at *m/z* 888.36 were observed and assigned as $AN_{139}CSAPCPQ$. However, there exists a 2 Da mass difference between observed peptide signal at *m/z* 888.36 and the theoretical sequence mass at *m/z* 890.35, which indicated that the two cysteines in ANCSAPCPQ may form a disulfide bond [30].

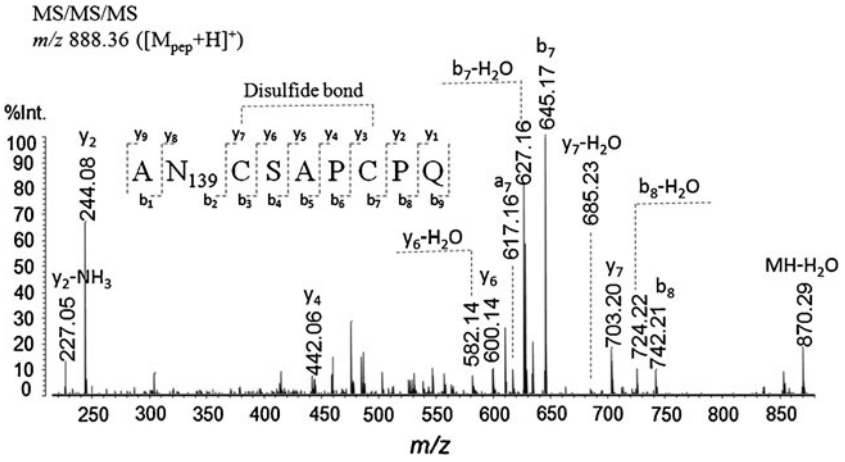

Fig. 3 MS^3 spectrum of *m/z* 888.36 of the Pronase E-digested glycopeptide of LOX-1, of which the peptide sequence is $AN_{139}CSAPCPQ$

The reduction of glycoprotein followed by alkylation was then employed prior to Pronase E digestion in order to verify the existence of a disulfide bond. Figure 4a shows the MS/MS spectrum of a Pronase E-digested glycopeptide at *m/z* 2626.18 after reduction and alkylation and its MS^3 spectrum of *m/z* 1264.18 corresponding to the $[M_{pep}+203+H]^+$ fragment (Fig. 4b). The b- and y- ions in Fig. 4b revealed that the peptide sequence was ANCSAPCPQD, which confirmed that Asn_{139} was the N-glycosylation site and explained the 2 Da mass differences between the observed and theoretical peptide

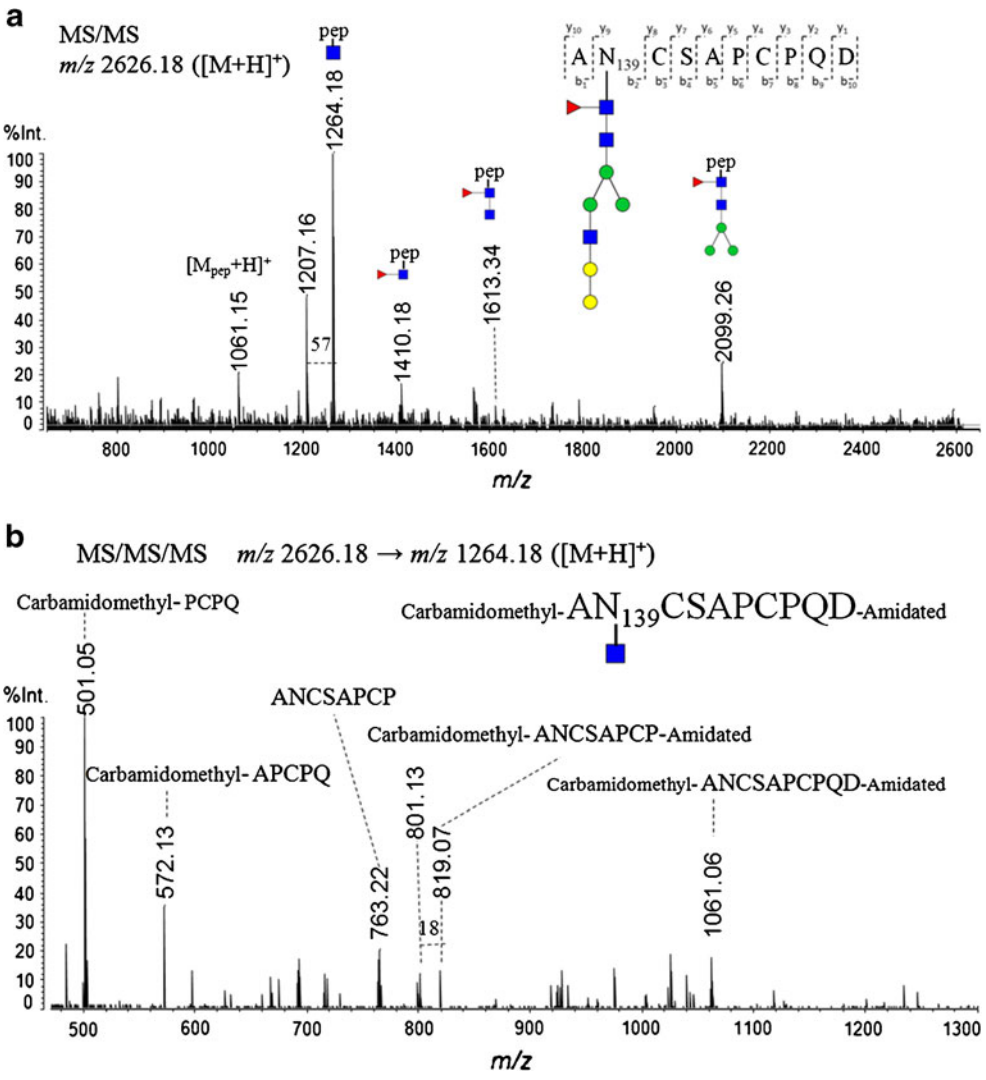

Fig. 4 MS/MS spectrum of a Pronase E-digested glycopeptide at *m/z* 2626.18 after reduction and alkylation (**a**) and MS^3 spectrum of *m/z* 1264.18 corresponding to the $[M_{pep}+203+H]^+$ fragment (**b**)

masses. Therefore, one glycosylation site at Asn_{139} of LOX-1 was identified by this method.

N-glycan structure determination from tandem MS spectra of glycopeptides

Subsequently, the mass of attached glycan moiety can be deduced by subtracting the backbone peptide mass obtained as above from the mass of its N-linked glycopeptide precursor. For example, a LOX-1 glycopeptide at *m/z* 3529.62 (Fig. 2b) yielded the peptide fragment mass of 910.18, of which the attached glycan mass was calculated as 2619. There were also two different series of fragment ions observed in Fig. 2b. The first series was similar to the one mentioned above in Fig. 2a and the second series of fragment ions (brown-colored in Fig. 2) was generated by Y-type and B-type cleavages of N-glycosidic linkages providing information about the glycan sequence, branching, and terminal motifs like N-glycan antennae structures [31–36]. The fragmentation nomenclature used here is described by Domon and Costello [37] where fragments containing a terminal (non-reducing end) sugar unit are termed A_i (cross-ring cleavages), B_i and C_i (glycosidic cleavages), whereas those fragments containing the aglycone (or the reducing sugar unit) are termed X_j (cross-ring), Y_j and Z_j (glycosidic) [37]. Subscripts indicate the position relative to the termini analogous to the system used in peptides, and the superscripts of cross-ring cleavage ions indicate the two bonds that are cleaved. Based on the following data we determined the composition of the glycan moiety and proposed the possible corresponding structures. According to the sequence of B- and Y- ions: $Y_{4\alpha'}Y_{4\alpha''}B_6$, $Y_{5\alpha'}Y_{4\alpha''}B_6$, $Y_{6\alpha'}Y_{4\alpha''}B_6$, $Y_{4\alpha''}B_6$, $Y_{5\alpha''}B_6$, $Y_{6\alpha''}B_6$, B_6, $Y_{1\gamma}{}^{0,2}A_7$ and ${}^{0,2}A_7$ at *m/z* 1239.16, 1442.21, 1604.20, 1766.19, 1696.23, 2131.23, 2293.22, 2413.22 and 2559.28, respectively, the composition of the N-glycan attached to the glycopeptide at *m/z* 3529.62 was 9 Hex, 1 core Fuc and 5 *N*-aceylglucosamine residues. There were two consecutive losses of 527 directly from the quasimolecular ion (*m/z* 3529.62→3002.30→2475.37), indicating that two same motifs of Hex-Hex-HexNAc were at non-reducing terminal positions. There is a direct Hex-Hex-HexNAc series loss from the quasimolecular ion (*m/z* 3529.62→3367.21→3205.17→3002.30), suggesting that the two Hex are external. Another direct loss of 146 from the quasimolecular ion (*m/z* 3529.62→3383.30) resulted from the labile nature of fucose and was followed by two consecutive losses of 527 (*m/z* 3383.30→2856.24→2329.22), which confirmed the deduction above.

Verification and analyses of N-glycan structures in LOX-1 by MALDI-QIT-TOF-MS/MS

Although the N-linked glycan structures of LOX-1 were determined at the level of glycopeptides, the N-glycosylation pattern of LOX-1 has not been determined and reported before. As released N-glycans by PNGase F are more amenable to tandem MS than large glycopeptides and possibly produce more strong signals for glycan fragment ions, released glycans with PNGase F using tandem MS were characterized to verify the glycan structures deduced from the corresponding glycopeptides.

Figure 5 shows the positive ion mass spectrum of N-glycans of LOX-1 released by PNGase F and Supplemental Table 2 has listed all the identified N-glycan compositions and corresponding proposed structures with their MALDI positive ions masses, which were observed in Fig. 5. There were no sufficient materials available for a whole range of exoglycosidase digestions to conform the monosaccharide constituents identification. However, the glycobiology knowledge has suggested these as being galactose, GlcNAc, fucose and mannose leaving little doubt as to the further identity of these residues of LOX-1 here.

Figure 6 shows the MALDI positive ion MS/MS of a triantennary N-linked glycopeptides at *m/z* 2660.52 (Supplemental Table 2, No. 13), the oligosaccharide composition of which corresponds to one Fuc (on the reducing-terminal GlcNAc residue), nine Hex, and five HexNAc, which is consistent with the glycan molecular weight and composition we deduced from the glycopeptide at *m/z* 3529.62 (Fig. 2). Supplemental Table 3 has listed the corresponding compositions and proposed structures of all the fragment signals observed in Fig. 6.

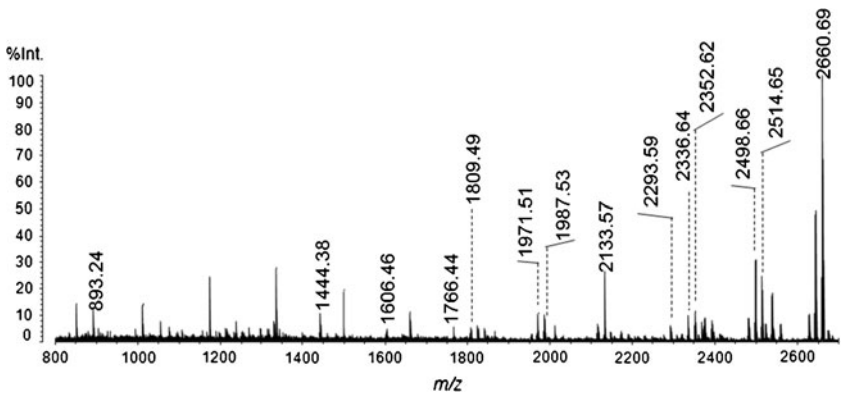

Fig. 5 MALDI-QIT-TOF-MS spectrum of PNGase F-released N-glycans of LOX-1

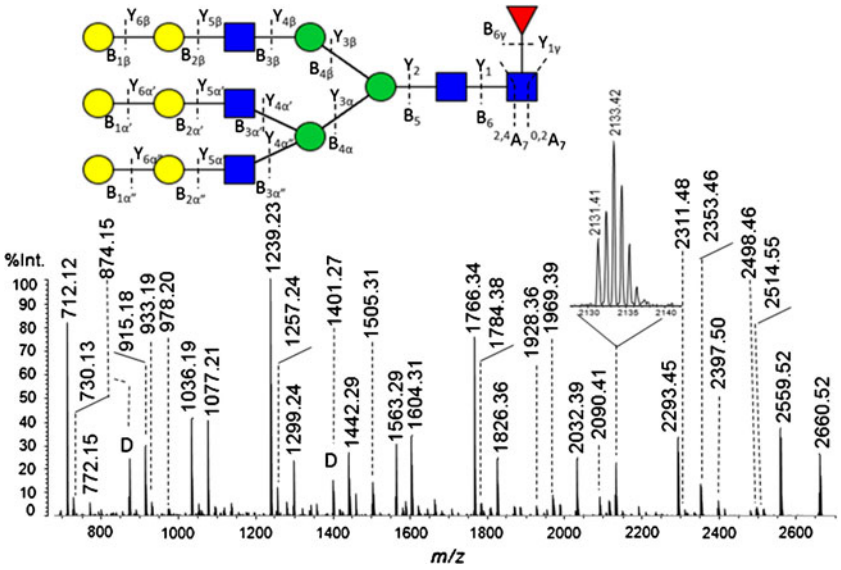

Fig. 6 MS/MS spectrum and structures with fragmentation nomenclature of the $[M+Na]^+$ of the PNGase F-released N-glycan with complex type structure at *m/z* 2660.52 of LOX-1

The 307 mass-unit loss (*m/z* 2660.52→2353.46) during the formation of $^{2,4}A_7$ ion revealed that fucose substitution was at the 6-position of the reducing-terminal GlcNAc residue, which was the summation of 146 (Fuc), 18 (H_2O) and 143 (part of the reducing-terminal GlcNAc by the cleavage of 2, 4 bonds) [38].

Three consecutive loss of 527 (*m/z* 2293.45→1766.34→1239.23→712.12) as predominant fragment ions was observed in the N-glycan MS/MS spectrum (Fig. 5), which verified that there were three Hex-Hex-HexNAc motifs at the non-reducing terminal. It is noted that the other two direct losses of Fuc (*m/z* 2660.52→2514.55) and 101 (part of the reducing-terminal GlcNAc by the cleavage of 0, 2 bonds, *m/z* 2660.52→2559.52) from the same quasimolecular ion occur by two different pathways: (1) the former is followed by the loss of 211 (HexNAc+H_2O) and forms the ion at m/z 2293.45, after which a series loss of 527 as described before occurs (*m/z* 2514.55→2293.45→1766.34→1239.23→712.12); (2) the latter is directly followed by the loss of 162 and the subsequent loss of 365 (Hex-HexNAc), which again confirms that the 527 motif sequence from the non-reducing terminal to the reducing terminal is Hex-Hex-HexNAc (*m/z* 2559.52→2397.50→2032.39→1505.31→978.20). The proposed composition of Hex-Hex-HexNAc is Gal-Gal-GlcNAc, which is unreasonable in human glycoprotein, but the LOX-1 studied in our study was expressed in murine myeloma cell line, which makes it possible for having Gal-Gal at the nonreducing end [39]. Two D ions at *m/z* 874.15 and 1401.27, respectively, in the spectrum of the tri-antennary glycan (Fig. 6) confirmed that the major isomer was a glycan containing a branched 3-antenna while the branched 6-anterna as minor. The predominant D ion at *m/z* 874.15 revealed Hex-Hex-HexNAc (Gal-Gal-GlcNAc) as the composition of the 6-antenna leaving the same composition for 3-antenna when it came to 1401.27 which was of low relative abundance. Additionally, it is known that the tri-antennary glycans were mainly branched on the 3-antenna rather than on the 6-arm [40–43]. Thus the released glycan structure analysis support the results we obtained from the method based on nonspecific digested glycopeptides analysis.

N-glycosylation status of Asn_{73}

Theoretically, there exist two potential N-glycosylation sites of LOX-1. Unfortunately, in our study, only one glycosylation site at Asn_{139} of LOX-1 was identified. In order to verify the occurrence of N-glycosylation at the other potential site Asn_{73}, both LOX-1 and deglycosyled LOX-1 incubated with PNGase F first were subject to SDS-PAGE. The changes in protein migration after enzymatic deglycosylation are shown in Fig. 7a. The resulting change in molecular weight could be detected as shifts in gel mobility, which allows us to get a general idea of the glycosylation status of LOX-1. Thus, compared to band 3 in lane 2, band 1 and 2 in lane 1 (Fig. 7a) are both glycosylated, which indicates there are two glycosylation forms of LOX-1.

PNGase F cleaves the linkage between GlcNAc and asparagines and converts Asn into Asp, and the resulting mass difference of 0.98 Da could be subsequently used to identify glycosylation sites by mass spectrometry [10]. Thus, excised band 1 and 2 were treated consecutively with PNGase F and trypsin after reduction and alkylation. The obtained PNGase F treated and tryptic peptides of LOX-1 were then analyzed by MALDI MS and MS/MS. The corresponding MALDI mass spectra of trypsin-digested peptides extracted from band 1 and 2 are shown in Fig. 7a and b, respectively and the tryptic

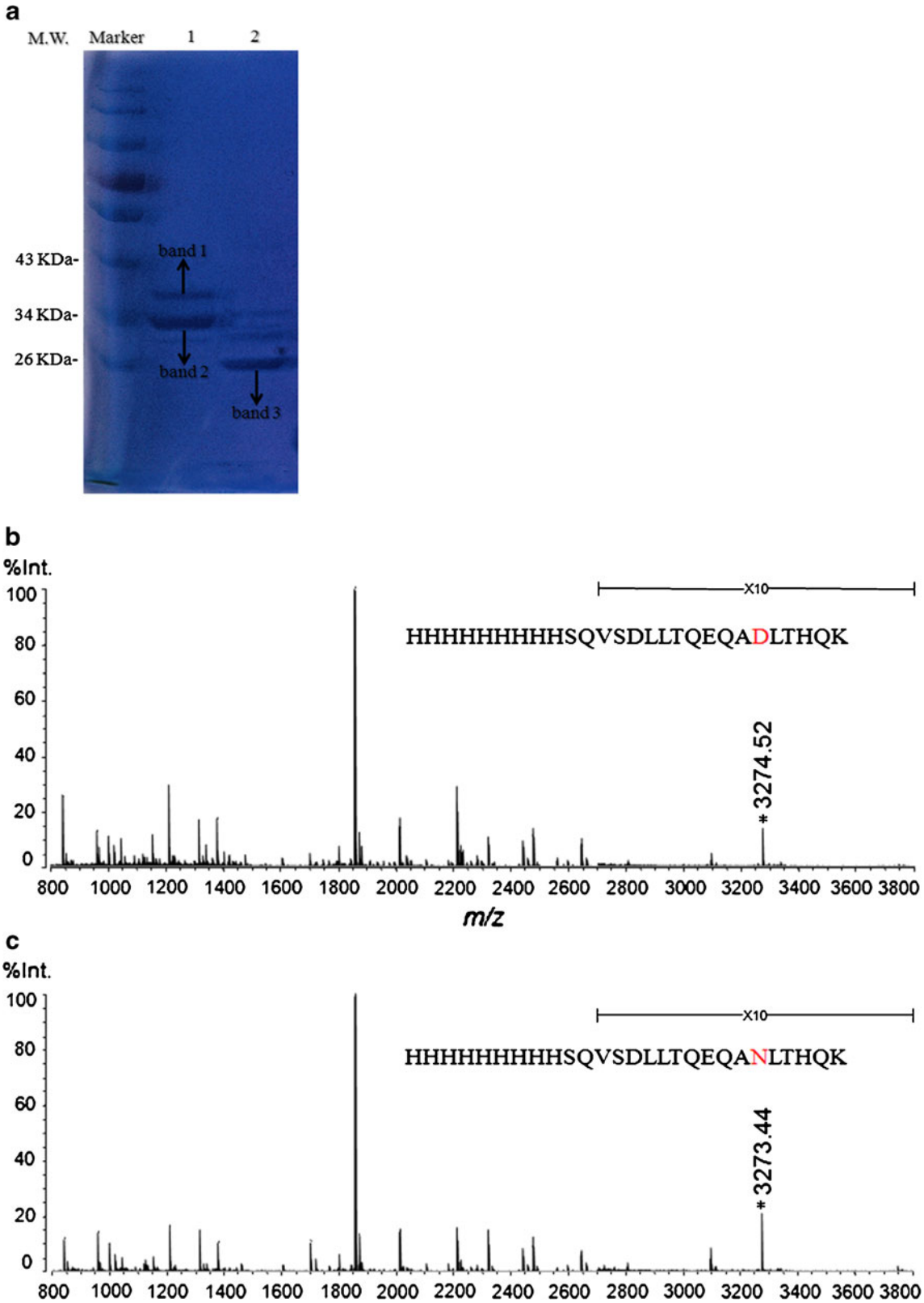

Fig. 7 SDS-PAGE separation of LOX-1 (**a**); lane 1: LOX-1; lane 2: deglycosylated LOX-1 incubated with PNGase F first; MALDI-QIT-TOF-MS spectra of trypsin-digested peptides of deglycosylated LOX-1 extracted from band 1 (**b**) and band 2 (**c**). The peptides containing Asn_{73} are marked with asterisks

peptides containing deglycosylated Asn_{73} are marked with asterisks. It was noted that glycosylation at Asn_{73} was only detected in band 1 but not in band 2. Furthermore, band 2 is observed as being more heavily stained with Coomassie blue than band 1 in Fig. 7a, which reveals that the nonglycosylated Asn_{73} is more abundant than the glycosylated ones. So the glycosylation of Asn_{73} was not detected previously, which may due to the low abundance of Asn_{73} glycosylated peptides. The corresponding MS/MS spectra of *m/z* 3274.54 and 3273.41 are shown in Supplemental Figure 1. However, the PNGase F treated and trypsin digested peptides containing the identified N-glycosylation site Asn_{139} were not detected in Fig. 7b or c, probably due to the large peptide mass (Supplemental Table 1), which further validates the advantages of non-specific digestion of LOX-1 mentioned previously.

Conclusion

In summary, nonspecific digestion with Pronase E can efficiently digest recombinant human LOX-1 to short glycopeptides amenable for tandem MS, allowing obtaining N-glycans composition information, while MS^3 enables the correct identification of the sequence for peptides portion of a glycopeptide. With the method employing Pronase E digestion combined with MALDI multistage MS, Asn_{139} of recombinant human LOX-1 has been revealed as an N-glycosylation site with corresponding complex type N-glycans attached, of which N-glycan compositions and deduced structures have been shown for the first time. Therefore, the method explored here is demonstrated to identify site-specific N-glycosylation simultaneously, which is promising as a simple and rapid approach to reveal the N-glycosylation pattern of the LOX-1. In addition, fragment pattern and diagnostic ions resulting from CID of nonspecific digested glycopeptides using MALDI-QIT-TOF-MS are discussed in detail, which could provide useful information for other similar work.

The determination of N-glycosylation in our study has laid the foundation for thorough research of the structure-biological function relationships of LOX-1. Furthermore, the nonspecific digestion method coupled with multistage MS techniques only requires trace amount of glycoproteins and could be applicable to the N-glycosylation characterization of endogenous human LOX-1, which is the subject of our further research.

Acknowledgments We gratefully acknowledge the financial support from National natural science fund (31100586, 31010103906, 30930025), National Basic Research Program of China (973 Program) (2012CB8221004, 2011CB910604) and National High-tech R&D Program (863 Program) (2012AA020203).

References

1. Ross, R.: The pathogenesis of atherosclerosis: a perspective for the 1990s. Nature **362**, 801–809 (1993)
2. Witztum, J.L., Steinberg, D.: Role of oxidized low density lipoprotein in atherogenesis. J. Clin. Invest. **88**, 1785–1792 (1991)
3. Sawamura, T., Kume, N., Aoyama, T., Moriwaki, H., Hoshikawa, H., Aiba, Y., Tanaka, T., Miwa, S., Katsura, Y., Kita, T., Masaki, T.: An endothelial receptor for oxidized low-density lipoprotein. Nature **386**, 73–77 (1997)
4. Kataoka, H., Kume, N., Miyamoto, S., Minami, M., Murase, T., Sawamura, T., Masaki, T., Hashimoto, N., Kita, T.: Biosynthesis and post-translational processing of lectin-like oxidized low density lipoprotein receptor-1 (LOX-1). N-linked glycosylation affects cell-surface expression and ligand binding. J. Biol. Chem. **275**, 6573–6579 (2000)
5. Apweiler, R., Hermjakob, H., Sharon, N.: On the frequency of protein glycosylation, as deduced from analysis of the SWISS-PROT database. Biochim. Biophys. Acta **1473**, 4–8 (1999)
6. Varki, A.: Biological roles of oligosaccharides: all of the theories are correct. Glycobiology **3**, 97–130 (1993)
7. Moens, S., Vanderleyden, J.: Glycoproteins in prokaryotes. Arch. Microbiol. **168**, 169–175 (1997)
8. Dennis, J.W., Granovsky, M., Warren, C.E.: Protein glycosylation in development and disease. Bioessays **21**, 412–421 (1999)
9. Grunewald, S., Matthijs, G., Jaeken, J.: Congenital disorders of glycosylation: a review. Pediatr. Res. **52**, 618–624 (2002)
10. Geyer, H., Geyer, R.: Strategies for analysis of glycoprotein glycosylation. Biochim. Biophys. Acta **1764**, 1853–1869 (2006)
11. Medzihradszky, K.F.: Characterization of protein N-glycosylation. Methods Enzymol. **405**, 116–138 (2005)
12. Budnik, B.A., Lee, R.S., Steen, J.A.: Global methods for protein glycosylation analysis by mass spectrometry. Biochim. Biophys. Acta **1764**, 1870–1880 (2006)
13. Dalpathado, D.S., Desaire, H.: Glycopeptide analysis by mass spectrometry. Analyst **133**, 731–738 (2008)
14. Wuhrer, M., Koeleman, C.A., Hokke, C.H., Deelder, A.M.: Protein glycosylation analyzed by normal-phase nano-liquid chromatography–mass spectrometry of glycopeptides. Anal. Chem. **77**, 886–894 (2005)
15. Wang, P., Li, G., Granados, R.R.: Identification of two new peritrophic membrane proteins from larval Trichoplusia ni: structural characteristics and their functions in the protease rich insect gut. Insect Biochem. Mol. Biol. **34**, 215–227 (2004)
16. Godl, K., Johansson, M.E., Lidell, M.E., Morgelin, M., Karlsson, H., Olson, F.J., Gum Jr., J.R., Kim, Y.S., Hansson, G.C.: The N terminus of the MUC2 mucin forms trimers that are held together within a trypsin-resistant core fragment. J. Biol. Chem. **277**, 47248–47256 (2002)
17. Barratt, J., Smith, A.C., Feehally, J.: The pathogenic role of IgA1 O-linked glycosylation in the pathogenesis of IgA nephropathy. Nephrology (Carlton) **12**, 275–284 (2007)
18. Larsen, M.R., Hojrup, P., Roepstorff, P.: Characterization of gel-separated glycoproteins using two-step proteolytic digestion combined with sequential microcolumns and mass spectrometry. Mol. Cell. Proteomics **4**, 107–119 (2005)
19. Sweeney, P.J., Walker, J.M.: Pronase (EC 3.4.24.4). Methods Mol. Biol. **16**, 271–276 (1993)
20. An, H.J., Peavy, T.R., Hedrick, J.L., Lebrilla, C.B.: Determination of N-glycosylation sites and site heterogeneity in glycoproteins. Anal. Chem. **75**, 5628–5637 (2003)
21. Yu, Y.Q., Fournier, J., Gilar, M., Gebler, J.C.: Identification of N-linked glycosylation sites using glycoprotein digestion with pronase prior to MALDI tandem time-of-flight mass spectrometry. Anal. Chem. **79**, 1731–1738 (2007)

22. Froehlich, J.W., Barboza, M., Chu, C., Lerno, L.A., Jr., Clowers, B.H., Zivkovic, A.M., German, J.B., Lebrilla, C.B.: Nano-LC-MS/MS of glycopeptides produced by nonspecific proteolysis enables rapid and extensive site-specific glycosylation determination. Anal. Chem. **83**, 5541–5547
23. Carlstedt, I., Lindgren, H., Sheehan, J.K.: The macromolecular structure of human cervical-mucus glycoproteins - studies on fragments obtained after reduction of disulfide bridges and after subsequent trypsin digestion. Biochem. J. **213**, 427–435 (1983)
24. Asker, N., Axelsson, M.A.B., Olofsson, S.O., Hansson, G.C.: Dimerization of the human MUC2 mucin in the endoplasmic reticulum is followed by a N-glycosylation-dependent transfer of the mono- and dimers to the Golgi apparatus. J. Biol. Chem. **273**, 18857–18863 (1998)
25. Ding, L., Kawatoh, E., Tanaka, K., Smith, A.J., Kumashiro, S.: High efficiency MALDI-QIT-ToF mass spectrometer. In: Munro, E. (ed.) Charged Particle Optics Iv, vol. 3777. Proceedings of the Society of Photo-Optical Instrumentation Engineers (Spie), pp. 144–155 (1999)
26. Martin, R.L., Brancia, F.L.: Analysis of high mass peptides using a novel matrix-assisted laser desorption/ionisation quadrupole ion trap time-of-flight mass spectrometer. Rapid Commun. Mass Spectrom. **17**, 1358–1365 (2003)
27. Neue, K., Mormann, M., Peter-Katalinic, J., Pohlentz, G.: Elucidation of glycoprotein structures by unspecific proteolysis and direct nanoESI mass spectrometric analysis of ZIC-HILIC-enriched glycopeptides. J. Proteome Res. **10**, 2248–2260
28. Wuhrer, M., Catalina, M.I., Deelder, A.M., Hokke, C.H.: Glycoproteomics based on tandem mass spectrometry of glycopeptides. J. Chromatogr. B Analyt. Technol. Biomed. Life Sci. **849**, 115–128 (2007)
29. Wu, Y., Mechref, Y., Klouckova, I., Mayampurath, A., Novotny, M.V., Tang, H.: Mapping site-specific protein N-glycosylations through liquid chromatography/mass spectrometry and targeted tandem mass spectrometry. Rapid Commun. Mass Spectrom. **24**, 965–972
30. Gorman, J.J., Wallis, T.P., Pitt, J.J.: Protein disulfide bond determination by mass spectrometry. Mass Spectrom. Rev. **21**, 183–216 (2002)
31. Uematsu, R., Furukawa, J., Nakagawa, H., Shinohara, Y., Deguchi, K., Monde, K., Nishimura, S.: High throughput quantitative glycomics and glycoform-focused proteomics of murine dermis and epidermis. Mol. Cell. Proteomics **4**, 1977–1989 (2005)
32. Wuhrer, M., Hokke, C.H., Deelder, A.M.: Glycopeptide analysis by matrix-assisted laser desorption/ionization tandem time-of-flight mass spectrometry reveals novel features of horseradish peroxidase glycosylation. Rapid Commun. Mass Spectrom. **18**, 1741–1748 (2004)
33. Kurogochi, M., Nishimura, S.: Structural characterization of N-glycopeptides by matrix-dependent selective fragmentation of MALDI-TOF/TOF tandem mass spectrometry. Anal. Chem. **76**, 6097–6101 (2004)
34. Krokhin, O., Ens, W., Standing, K.G., Wilkins, J., Perreault, H.: Site-specific N-glycosylation analysis: matrix-assisted laser desorption/ionization quadrupole-quadrupole time-of-flight tandem mass spectral signatures for recognition and identification of glycopeptides. Rapid Commun. Mass Spectrom. **18**, 2020–2030 (2004)
35. Bykova, N.V., Rampitsch, C., Krokhin, O., Standing, K.G., Ens, W.: Determination and characterization of site-specific N-glycosylation using MALDI-Qq-TOF tandem mass spectrometry: case study with a plant protease. Anal. Chem. **78**, 1093–1103 (2006)
36. Takemori, N., Komori, N., Matsumoto, H.: Highly sensitive multistage mass spectrometry enables small-scale analysis of protein glycosylation from two-dimensional polyacrylamide gels. Electrophoresis **27**, 1394–1406 (2006)
37. Domon, B., Costello, C.E.: A systematic nomenclature for carbohydrate fragmentations in FAB-MS MS spectra of glycoconjugates. Glycoconj. J. **5**, 397–409 (1988)
38. Harvey, D.J.: Fragmentation of negative ions from carbohydrates: part 3. Fragmentation of hybrid and complex N-linked glycans. J. Am. Soc. Mass Spectrom. **16**, 647–659 (2005)
39. Montesino, R., Toledo, J.R., Sanchez, O., Zamora, Y., Barrera, M., Royle, L., Rudd, P.M., Dwek, R.A., Harvey, D.J., Cremata, J.A.: N-glycosylation pattern of E2 glycoprotein from classical swine fever virus. J. Proteome Res. **8**, 546–555 (2009)
40. Harvey, D.J., Bateman, R.H., Green, M.R.: High-energy collision-induced fragmentation of complex oligosaccharides ionized by matrix-assisted laser desorption/ionization mass spectrometry. J. Mass Spectrom. **32**, 167–187 (1997)
41. Harvey, D.J.: Structural determination of N-linked glycans by matrix-assisted laser desorption/ionization and electrospray ionization mass spectrometry. Proteomics **5**, 1774–1786 (2005)
42. Harvey, D.J., Baruah, K., Scanlan, C.N.: Application of negative ion MS/MS to the identification of N-glycans released from carcinoembryonic antigen cell adhesion molecule 1 (CEACAM1). J. Mass Spectrom. **44**, 50–60 (2009)
43. Harvey, D.J., Martin, R.L., Jackson, K.A., Sutton, C.W.: Fragmentation of N-linked glycans with a matrix-assisted laser desorption/ionization ion trap time-of-flight mass spectrometer. Rapid Commun. Mass Spectrom. **18**, 2997–3007 (2004)